The Behavior of the Modal Properties of Weak and Strong Coupled Acoustic Modes at Different Pressure Levels in a Rotor-Stator Test Rig

Botond Barabas, Dieter Brillert, Hans Josef Dohmen, Friedrich-Karl Benra

The Behavior of the Modal Properties of Weak and Strong Coupled Acoustic Modes at Different Pressure Levels in a Rotor-Stator Test Rig

Botond Barabas[1]*, Dieter Brillert[1], Hans Josef Dohmen[1], Friedrich-Karl Benra[1]

ISROMAC 2017

International Symposium on Transport Phenomena and Dynamics of Rotating Machinery

Hawaii, Maui

December 16-21 2017

Abstract

The application of high pressure radial compressors is expected to have an above-average growth rate in future. When vibrations are matter of investigations, impellers surrounded by dense gases cannot be treated separately but as a coupled system comprising the impeller structure and the fluid.

In this paper experimental results gathered in a rotor-stator test rig at different gas pressures are presented. The modal properties of a weakly coupled acoustic mode and a strongly coupled acoustic mode are determined. The results show no influence of the gas pressure on the natural frequency of the weakly coupled acoustic mode. The damping of it is approaching a minimum with increasing gas density. The natural frequencies of the strongly coupled modes diverge from each other when the gas pressure is increased.

Keywords

Natural frequency — Coupled modes — Aerodynamic damping

[1] *Chair of Turbomachinery, University of Duisburg-Essen, Duisburg, Germany*

***Corresponding author**: botond.barabas@uni-due.de

NOMENCLATURE

Latin symbols		
b, *s*	[m]	Thickness of disk, axial gap width
c	[m/s]	Speed of sound
f, *f**	[1/s], [-]	Frequency, dimensionless frequency in relation to the acoustic dominant natural frequency (m_{ac} = 4, n_{ac} = 0, l_{ac} = 1)
l	[-]	Axial order (number of axial nodes)
m	[-]	Circumferential order (number of node diameters)
n	[-]	Radial order (number of node circles)
p	[bar]	Pressure
$S_{max,exc}$	[Hz/s]	Maximum sweep velocity
Greek symbols		
α	[°]	Angle in circumferential direction
ρ	[kg/m^3]	Density
v	[m^2/s]	Kinematic viscosity
Δ*ω*, *ω*	[1/s]	Frequency difference in radian, frequency in radian
*ζ**	[-]	Dimensionless critical damping ratio related to the critical damping ratio of the acoustic dominant mode (m_{ac} = 4, n_{ac} = 0, l_{ac} = 1))
Indices		
ac		Acoustic
f		Fluid
r		Resonance
st		Structure

INTRODUCTION

High pressure radial compressors are expected to have an above-average growth rate in future. The main application fields of these machines are at oil exploitation sites as re-injection gas supplies or at Carbon-Capture-and-Storage power plants for carbon dioxide compression. The operational pressures and densities of the working fluids are intended to increase with these applications. Together with the increasing fluid density, aeroacoustics and aeroelasticity have a great impact when it comes to vibration issues and high cycle fatigue. Especially, the aeroacoustics in the side cavities of radial compressors play a major role in the operational reliability of radial compressors.

One of the first publications about a fundamental aeroacoustic excitation source in turbomachines has been published by Tyler and Sofrin [1]. They reveal excitations at discrete frequencies as an interaction between rotor and stator components, the so called Tyler-Sofrin modes. Ehrich [2] conducted further studies that he has focused on natural frequencies of acoustic modes in annular cavities influenced by axial flow and flow rotation. A problem orientated numerical investigation of acoustic modes in the side cavities of radial compressors has been conducted by König [3], who reveals a coupling of the acoustic modes in the two side cavities with each other. The paper compares 2D-analytical and 3D-FEM methods for acoustic mode calculations. Petry [4] has been the first who showed the excitation of acoustic resonances in side cavities of radial compressors with Tyler-Sofrin modes in his experiments.

When vibrations are matter of investigations, impellers surrounded by dense gases cannot be treated separately but

as a coupled system comprising the impeller structure and the fluid. Each nodal diameter natural mode is at least split into two modes with two corresponding natural frequencies. For a weak coupling the coupled natural frequencies approximately equal the uncoupled structural and acoustic natural frequencies, respectively. The stronger the coupling the merrier the coupled natural frequencies differ from the uncoupled ones.

The effect of dense surrounding fluids on the natural frequencies of pump impellers has been investigated numerically by Liang et al. [5] and experimentally by Rodriguez et al. [6]. They conducted their investigations by keeping the fluid pressure constant and changing the type of the fluid. Their findings are decreasing natural frequencies of the impeller and increasing damping ratios if the impeller is surrounded by water instead of air. Magara et al. [7] have investigated the natural frequencies of a radial compressor impeller for different surrounding gas pressures experimentally. For some natural frequencies of the structure their results show a decreasing trend for increased pressures; however, other natural frequencies increase at the same time. They conclude an influence of the stiffness of the surrounding gas beside the added mass effect onto the structure.

Sandberg and Göransson [8] have conducted a numerical finite element approach to investigate a coupled fluid-structure interaction of an aircraft fuselage. They have found striking differences between the uncoupled and coupled eigenfrequencies. In their numerical investigation of coupled eigenmodes of a nuclear vessel Sigrist et al. [9] discover a change of mode shapes at increasing fluid densities. This effect is observed in the results when added mass and coupling effects are taken numerically into account.

It becomes apparent that aeroelasticity and aeroacoustics in side cavities of radial compressors is a complex research field. Investigations in the past have revealed some effects, which cannot be fully described, yet. In order to gather fundamental understanding of these effects a rotor-stator test rig has been built up at the University of Duisburg-Essen. The main advantage of its design is that contrary to real compressors the excitation frequency and strength can be set independently from gas parameters and disk rotational speeds. This decoupling of excitation source and the system, which should be excited, allows the identification of influence parameters. Only a few publications [5, 6, 10] have investigated the influence of fluid density variations on the aerodynamic damping of disks in radial turbo machines. Though, a more thorough knowledge of the aerodynamic damping of acoustic and of structural modes could improve the operational reliability of high pressure radial compressors. In this paper the influence of the surrounding gas pressure variation on the damping and natural frequencies of weakly and strongly coupled acoustic modes are presented. The experimental data is gathered with a non-rotating disk.

1. EXPERIMENTAL SETUP AND METHODOLOGY

1.1 Test rig

The measurements presented in this paper are conducted in the rotor-stator test rig that has been introduced in the framework of aerodynamic and acoustic measurements in Barabas et al. [11, 12]. Geometrically, the test rig represents simplified side cavities of radial compressors. In Figure 1 one stage of a radial compressor is sketched. The side cavities are the spaces between the casing and the impeller's hub and shroud. They are marked green and blue in Figure 1, respectively. These cavities are simplified in the test rig (Figure 2). The impeller represented as a plain disk is embraced by a plain walled casing. To distinguish between the cavity where the loudspeakers excite the fluid and the most sensors are mounted this cavity is called the front cavity and the other rear cavity. The sensors' and loudspeaker's allocations are sketched in the figure, too. The axial gap widths (s) in both cavities can be adjusted independently from each other covering the range of gap widths of modern radial compressors. Within this experimental investigation the gap widths in both cavities are set equally. The disk thickness (b) has been chosen to enforce at least one pair of acoustic and structural modes, with the same number of nodal diameters, to have similar uncoupled natural frequencies at ambient conditions. This ensures a strong coupling between the acoustic and structure mode. Furthermore, the geometric dimensions of the cavities and the disk have been chosen in a way that other acoustic and structure natural frequencies with equal mode shapes differ from each other. This guarantees a weak coupling between those. A picture of the test rig, taken from the front cavity side, is presented in Figure 3.

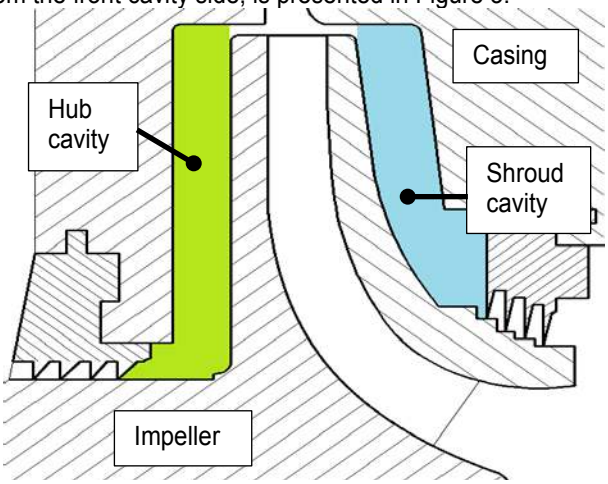

Figure 1. A meridional sketch of a radial compressor stage with the side cavities.

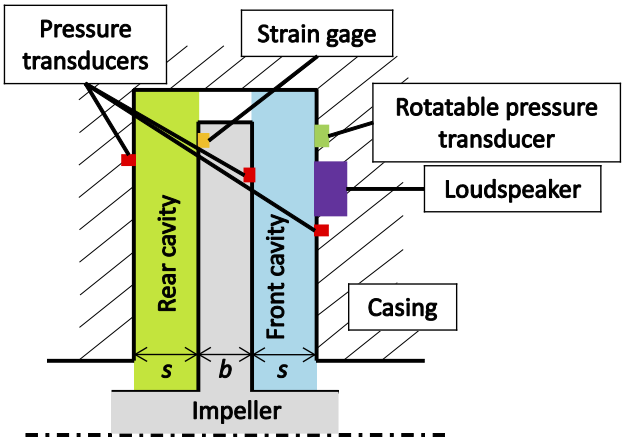

Figure 2. Sketch of the rotor-stator test rig with the acoustic specific instrumentation (meridional view).

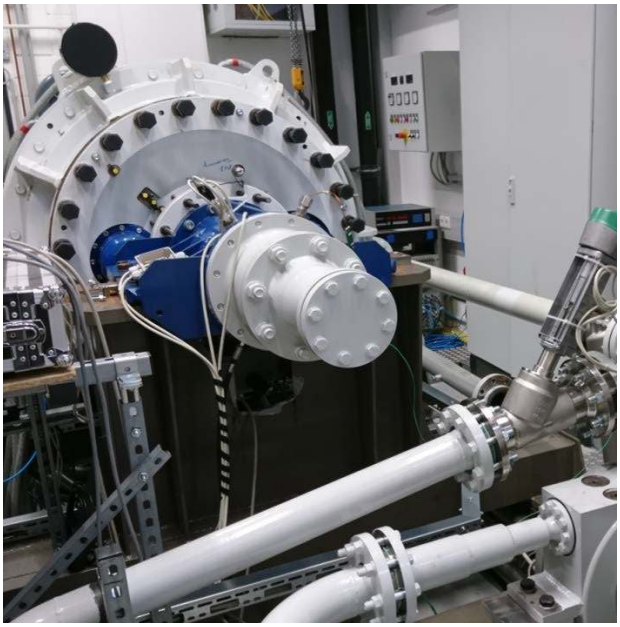

Figure 3. A picture of the test rig.

1.2 Instrumentation

The acoustic specific instrumentation of the test rig with the uncertainty and repeatability analysis is described in detail in Barabas et al. [12]. The test rig is equipped with loudspeakers as excitation sources to overcome the absence of blade-vane interaction. The applied acoustic specific pressure transducers and strain gages are summarized in Table 1. The transducer positions in meridional view and in normal view are presented in Figure 2 and Figure 4, respectively. However, even the identification of low order modes is an impossible task with a finite number of pressure transducers. As remedy, a novel rotatable pressure transducer has been developed and built in the front cavity casing of the test rig. It is based on an idea of rotatable microphones [13]. Together with a specific evaluation method the pressure pattern of an acoustic mode at a constant excitation frequency can be obtained in circumferential direction.

In Figure 4 the test rig is sketched in the normal view with the sensor positions. The pressure sensors are marked with a “P”, the strain gages with a “G”, and “LS” refers to the loudspeakers. The character inside the parentheses represents the location: The rear cavity is labeled with “RC” and the disk is labeled with “D”. If the location character is omitted the sensor is mounted in the front cavity. The presented results within this paper have been recorded with the pressure sensor “P147” and the strain gage “G142 (D)”, mounted on the disk. The fluid is excited with the loudspeaker “LS 2”. For a better differentiation they are marked red in the figure.

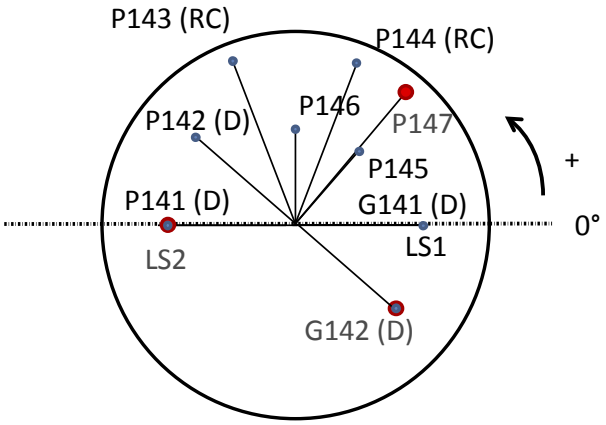

Figure 4. Normal view of the rotor-stator test rig with the sensors’ allocations. Within this paper results of the red marked sensors are presented. Labels: “P”: pressure sensor, “G”: strain gage, “LS”: loudspeaker, “RC”: rear cavity, “D”: disk

Table 1. Summary of the measurement instrumentation.

Installed location	Type of transducer	Quantity
Impeller	Strain gage	2
Impeller	Piezoresistive pressure transducer	2
Rear cavity	Piezoresistive pressure transducer	2
Front cavity	Piezoelectric pressure transducer	2
Front cavity (Rotatable transducer)	Piezoelectric pressure transducer	1

1.3 Methodology

Experimental Procedure and Boundary Conditions

The basis for the evaluation of the natural frequencies and the modal damping values are frequency sweep experiments over a specific interval. The maximum allowed sweep velocity $S_{\mathrm{max,exc}}$ without falsifying the measured resonance height, frequency, and damping is set according to Ewins [14] to

$$S_{\mathrm{max,exc}} = 3.6 \cdot f_r^2 \zeta^2 \qquad (1)$$

with f_r as the resonance frequency and ζ as the critical damping ratio.

The developed pressure patterns at certain frequencies

are measured with the rotatable pressure sensor in circumferential direction. The measurement procedures are described in Barabas et al. [12].

The experiments are conducted with air as fluid at different pressure levels. They are summarized in Table 2. The speed of sound changes due to the pressure increase less than 1% and is only considered for the weakly coupled acoustic mode.

Table 2. : Summary of the experimental boundary conditions.

Pressure level [bar]	Density [kg/m^3]	Speed of sound [m/s]
1	1.17	342.6
5	5.92	343.2
9	10.77	343.4
13	15.68	344.2
17	20.47	344.8

Evaluation Procedure

The measured data of the sweep experiments are evaluated with a Short Time Fourier Transformation (STFT) in Matlab®. The data blocks for the STFT have been chosen small enough to allow a good resolution in time. The overlap of 75% between two adjacent blocks avoids data loss. With the knowledge and application of the excitation frequency to time relation, a good frequency resolution can be achieved, too.

However, because the excitation force of the loudspeakers on the fluid cannot be determined directly it is assumed to be constant in the small frequency range around a resonance. Hence, the Frequency Response Function (FRF) is not calculated; instead, the analysis is based on the direct response of the transducers, not set in relation to the excitation force. Comparisons of the response signals' amplitude between different pressure levels should be treated with caution.

There are different methods to determine the modal parameters of a system. Each has its advantages and disadvantages for particular vibrating systems. In the framework of this paper the peak-amplitude method is applied, as presented in Ewins [14]. It can resolve the natural frequencies of the strongly coupled modes and the natural frequencies and the damping of the weakly coupled mode, because it is well separated from adjacent mode. Because the structural and mechanical damping is very small compared to the aerodynamic damping they are neglected within this paper.

Analytical approach

The experimental results of the natural frequencies are compared with a qualitative analytical approach presented by Magara et al. [15] to estimate the natural frequency shift of a similar coupled system with a disk enclosed in a gas cavity. They couple the equations of motions of the gas and the structure and assume an inviscid and compressible gas. They obtain

$$\left(\omega_{\mathrm{ac,r}}^2-\omega^2\right)\left(\omega_{\mathrm{st,r}}^2-\omega^2\right)-2\omega^2\frac{\rho_{\mathrm{f}}\cdot c^2}{\rho_{\mathrm{st}}\cdot bs}=0 \qquad (2)$$

with $\omega_{\mathrm{ac,r}}$ and $\omega_{\mathrm{st,r}}$ as the uncoupled natural frequencies with the same mode shape of the fluid and disk, respectively. ρ_{f} and ρ_{st} correspond to the density of the fluid and the structure. The fluid's speed of sound is denoted with *c* and the geometry is represented by *b* as the disk thickness and *s* as the axial gap width of the cavity (Figure 2). The minuend of Equation (2) can be graphically represented as a parabola, the subtrahend as a line. Two solutions exist at the cross-sections. These are the coupled natural frequencies of the system. Magara et al. [15] have introduced the terms "disc origin" and "fluid origin mode" for the respective branches of the parabola, depending on the uncoupled natural frequencies. The terms are renamed to "structure dominant" and "acoustic dominant" within this paper. The vibration can be characterized with the phase relation between the axial disk motion and the pressure pattern's resulting axial force onto the disk, too. In the model of Magara the lower frequency branch is called "in-phase mode" and the higher frequency branch "out-of-phase mode".

The uncoupled natural frequencies $\omega_{\mathrm{ac,r}}$ and $\omega_{\mathrm{st,r}}$ for Equation (2) cannot be determined directly from the measurements, because the modes with natural frequencies at f^* = 0.93 and at f^* = 1 are already strongly coupled. Therefore, the uncoupled natural frequencies are determined via solving Equation (2) with the experimental data from the 1 bar case. The resulting values for the uncoupled natural frequencies $\omega_{\mathrm{ac,r}}$ and $\omega_{\mathrm{st,r}}$ are used to calculate the natural frequencies at higher gas densities.

2. RESULTS AND DISCUSSION

In this part the results of the weakly and strongly coupled modes are presented. This paragraph starts with the results for the weakly coupled mode and thereafter the results for the strongly coupled acoustic mode are presented.

2.1 Weakly coupled mode

The mode that has been chosen for the investigation of the weakly coupled mode has a natural frequency of f^* = 0.97 at ambient conditions. The response of the pressure sensor at ambient conditions is presented in Figure 5. A peak is visible at the non-dimensional frequency f^* = 0.97. On the contrary, the response of the strain gage mounted on the disk (Figure 6) does not show a pronounced response at the non-dimensional frequency f^* = 0.97. Thus, the coupling between the fluid and structure is very weak; furthermore, the excited mode is an acoustic mode.

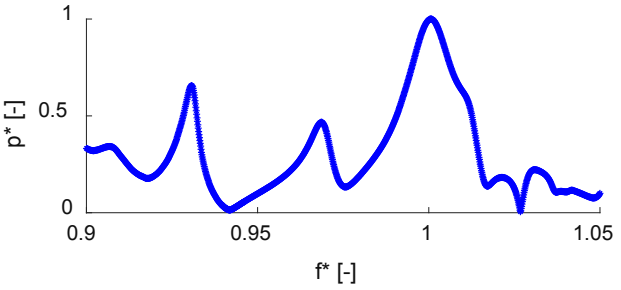

Figure 5. STFT result of the frequency sweep at ambient conditions (pressure sensor data, P147).

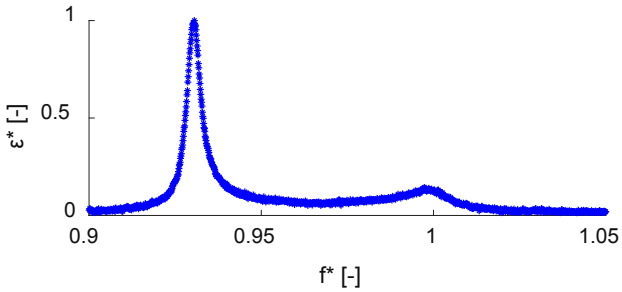

Figure 6. STFT result of the frequency sweep at ambient conditions (strain gage data, G142).

The pressure pattern in circumferential direction of the acoustic dominant mode is presented in Figure 7. The data is recorded with the rotatable pressure sensor as introduced in Barabas et al. [12] and shows the envelope of the pressure at different circumferential positions for two opposite chronological phases (0 and π). The pressure pattern is a superposition of an acoustic mode with zero and five nodal diameters. Due to this superposition only two nodes can be identified where the envelopes of both phases cross each other. This is at a circumferential position of 90° and 120°. If the superpositioned mode with zero nodal diameters was not present, the pressure envelopes would additionally cross each other at 10°, 40°, and 170° circumferential position. The five nodes between 0° and 180° circumferential position can be determined from the time-sequence animation.

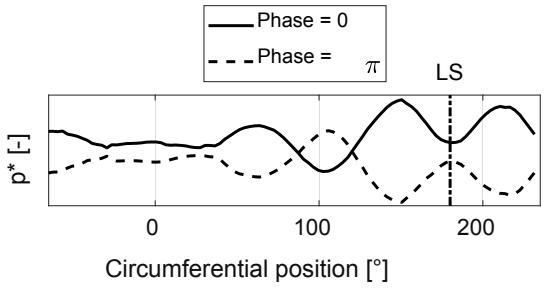

Figure 7. Results of the rotatable pressure sensor at f* = 0.97, the weakly coupled mode.

The influence of the surrounding gas density on the natural frequency of the weakly coupled mode is presented in Figure 8. Only a marginal influence of the increasing density on the natural frequency can be read from the diagram. It has to be pointed out, that the influence of the speed of sound cannot be neglected in this case. Therefore the natural frequency plotted in the diagram is compensated and related to the speed of sound at ambient conditions. However, the surrounding gas density does not influence the natural frequency of the acoustic dominant mode.

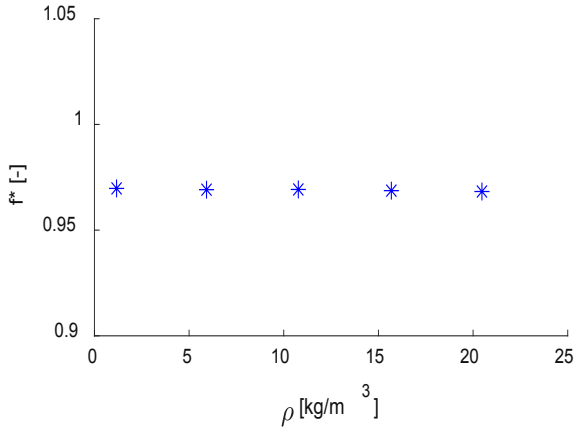

Figure 8. The natural frequency of the weakly coupled mode in dependence of the surrounding gas density. Compensated with the speed of sound.

In Figure 9 the STFT results of the acoustic dominant mode in dependence of the surrounding gas pressure are plotted over the non-dimensional frequency. The curves are compensated with the speed of sound. A difference between the case at 1 bar and the other gas pressure cases is obvious. The response amplitude of the 1 bar case is significantly lower and the peak is flatter than the respective properties of the other cases.

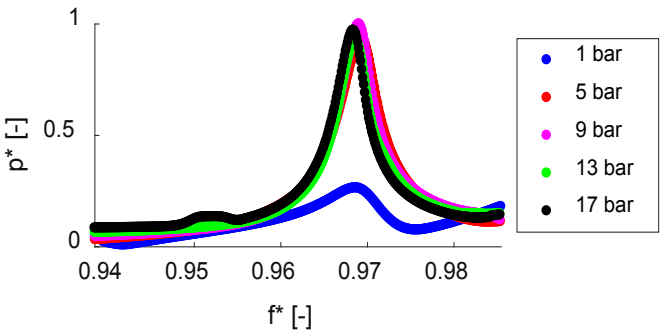

Figure 9. The STFT of the weakly coupled mode recorded with a pressure sensor in dependence of the surrounding gas pressure. Compensated with the speed of sound.

The damping is analyzed with the peak-amplitude method and the results are plotted in Figure 10. The apparent behavior from the qualitative STFT curves is confirmed with the peak-amplitude method. The damping decreases with increasing densities and approaches a minimum at a density around 11 kg/m^3. A further increase of the gas density does not influence the damping of the weakly coupled acoustic mode.

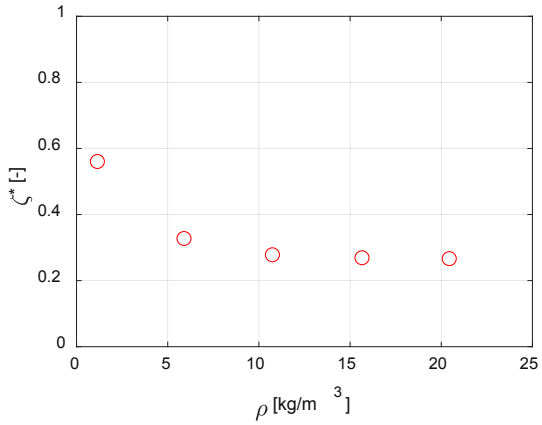

Figure 10. The damping of the weakly coupled mode in dependence of the surrounding gas density.

It is assumed, that the damping behavior of this particular mode is influenced by two effects that superpose each other. The first one is a generally decreasing damping ratio of weakly coupled acoustic mode with increasing gas density. The second one is the influence of an adjacent mode. This adjacent mode could be the already mentioned strongly coupled acoustic mode at a non-dimensional frequency of $f^* = 1$. The difference of the natural frequencies of both modes is the smallest for the 1 bar case. It increases, because the natural frequencies of the strongly coupled modes diverge from each other when the gas pressure is increased. The influence of the adjacent mode is hardly visible for a gas density higher than approximately 11 kg/m^3 where the damping nearly remains at a constant minimum level.

2.2 Strongly coupled mode

The strongly coupled modes that have been chosen for this investigation have a non-dimensional natural frequency $f^* = 0.93$ and $f^* = 1$. Their response peaks can be well recognized as peaks in the pressure sensor data in Figure 5, though the results of the strain gage in Figure 6 give a clearer result. Both modes can be observed in the data of both different transducer types, which means a strong coupling with each other. Based on the strain gage data the excited mode at $f^* = 0.93$ has a five times higher response amplitude as the excited mode at $f^* = 1$. Therefore, the mode with the lower natural frequency is the structure dominant mode and the mode with the higher natural frequency the acoustic dominant. The next step is the identification of the excited modes before the natural frequencies of the strongly coupled modes can be investigated in dependence of the gas density. The envelopes of the pressure pattern in dependence of the circumferential position are presented for the structure dominant mode ($f^* = 0.93$, Figure 11) and the acoustic dominant mode ($f^* = 1$, Figure 12). The pressure envelopes are based on the data from the rotatable pressure sensor. Four nodes over 180° in circumferential direction can be observed, respectively. Hence, the number of nodal diameters is m = 4. The pressure signals of the transducers in the front and rear cavity are in phase opposition to each other, this means the number of axial nodes is l = 1 and a net pressure force takes effect on the disk. The number of nodal circles can be determined with n = 0, due to the in-phase signal of the outer and inner pressure transducer.

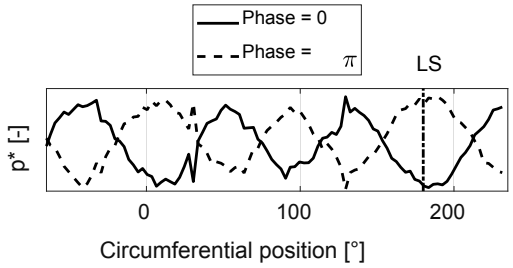

Figure 11. Results of the rotatable pressure sensor at $f^* = 0.93$, the structure dominant mode.

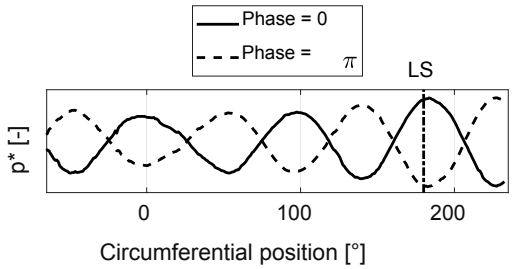

Figure 12. Results of the rotatable pressure sensor at $f^* = 1$, the acoustic dominant mode.

The variation of the surrounding gas pressure shifts both natural frequencies, the one of the acoustic dominant as well as the one of the structure dominant mode. This phenomenon has been shown by Magara et al. [15] and repeated in former experiments in the test rig at lower gas pressures (Barabas et al. [12]). In Figure 13 the measured and the analytically determined natural frequencies (Magara [15]) are plotted over the gas density. They show qualitatively the same diverging behavior for the acoustic and structure dominant mode when the surrounding gas pressure is increased. Towards higher densities the measured acoustic dominant natural frequencies show a deviation from the calculated ones. On the first sight, the analytical and the measured natural frequencies of the structure dominant mode appear to fit well.

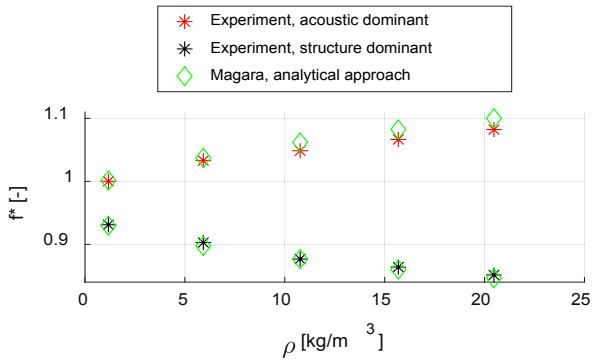

Figure 13. Frequency shift due to pressure variation

CONCLUSIONS AND OUTLOOK

In this paper the modal properties of a weakly coupled acoustic mode and a strongly coupled acoustic and structure mode are presented. The vicinity of the strongly coupled acoustic mode at low gas pressures is most likely the reason for the higher damping of the weakly coupled acoustic mode

until $\rho = 11\ kg/m^3$. For this particular weakly damped acoustic mode it may be concluded that the damping is influenced by a close mode but not by the increasing density of the fluid, whereas the natural frequency of it is neither influenced by the vicinity of a mode nor by the increasing density of the fluid

The increase of the surrounding gas pressure lets the natural frequencies of the strongly coupled acoustic and structure modes diverge from each other.

In the future, the detected effects within this paper should be analyzed more intensively. The findings that have been made for a particular mode are going to be analyzed for the general case. The knowledge about adjacent modes that influence each other's damping needs a more thorough investigation. Furthermore, the influence of disk rotation on the behavior of the modal properties will be investigated in future experimental campaigns. Those results could be applied in the design of radial compressors and if the aerodynamic damping behavior is understood better, the operational reliability of radial compressors could be improved.

ACKNOWLEDGMENTS

This project is funded by BMWi (Bundesministerium für Wirtschaft und Energie). The authors are grateful for the financial support under contract number 03ET2011E.

REFERENCES

[1] J. M. Tyler, T. G. Sofrin. Axial Flow Compressor Noise Studies. *SAE Transactions*, 70:309-332, 1961.

[2] F.F. Ehrich. Acoustic Resonances and Multiple Pure Tone Noise in Turbomachinery Inlets. *ASME Journal of Engineering for Power*, 91:253-262, 1969.

[3] S König. Acoustic Eigenmodes in the Side Cavities of Centrifugal Compressors. *Proceedings of ASME Turbo Expo*, Orlando, Florida, USA, GT2009-59650, 2009.

[4] N. Petry. Experimentelle Untersuchung aero-akustischer und aeroelastischer Phänomene in Hochdruck-Radialverdichtern. *Ph.D. Dissertation, Universität Duisburg-Essen*, Essen, Germany, 2011.

[5] Q. W. Liang, C. G. Rodríguez, E. Egusquiza, X. Escaler, M. Farhat, F. Avellan. Numerical simulation of fluid added mass effect on a francis turbine runner. *Computers & Fluids*, 36:1106-1118, 2007.

[6] C. G. Rodriguez, E. Egusquiza, X. Escaler, Q. W. Liang, F. Avellan. Experimental investigation of added mass effects on a Francis turbine runner in still water. *Journal of Fluids and Structures,* 22:699-712, 2006.

[7] Y. Magara, K. Yamaguchi, H. Miura, N. Takahashi, M. Narita. Natural Frequency Shift in a Centrifugal Compressor Impeller for High-Density Gas Applications. *Journal of Turbomachinery*, 135:011014-1–011014-8, 2013.

[8] G. Sandberg, P. Göransson. A Symmetric Finite Element Formulation for Acoustic Fluid-Structure Interaction Analysis. *Journal of Sound and Vibration*, 123:507-515, 1988.

[9] J.-F. Sigrist, D. Broc, C. Lainé. Dynamic analysis of a nuclear reactor with fluid-structure interaction Part I: Seismic loading, fluid added mass and added stiffness effects. *Nuclear Engineering and Design*, 236:2431-2443, 2006.

[10] B. Beirow, T. Maywald, A. Kühhorn. Mistuning and Damping Analysis of a Radial Turbine Blisk in Varying Ambient Conditions. *Proceedings of ASME Turbo Expo*, Düsseldorf, Germany, GT2014-25521, 2014.

[11] B. Barabas, S. Clauss, S. Schuster, F.-K. Benra, H. J. Dohmen, D. Brillert. Experimental and Numerical Determination of Pressure and Velocity Distribution Inside a Rotor-Stator Cavity at very High Circumferential Reynolds Numbers. *Proceedings of 11th European Turbomachinery Conference*, Madrid, Spain, 2015

[12] B. Barabas, D. Brillert, H. J. Dohmen, F.-K. Benra. Identification of Coupled Natural Frequencies in a Rotor-Stator Test-Rig for Different Gas Properties. *Proceedings of 12th European Conference on Turbomachinery Fluid dynamics & Thermodynamics,* Stockholm, Sweden, ETC2017-057 2017.

[13] D. E. Cicon, T. G. Sofrin, D. C. Mathews. Investigation of Continuously Traversing Microphone System for Mode Measurement. *NASA*, 1982.

[14] D. J. Ewins. Modal Testing: Theory and Practice. *Research Studies Press*, 1995.

[15] Y. Magara, M. Narita, K. Yamaguchi, N. Takahashi, T. Kuwano. Natural Frequencies of Centrifugal Compressor Impellers for High Density Gas Applications. *IMECE2008*, Boston, Massachusetts, USA, IMECE2008-67278, 2008.